ISSN 1063-7729, Astronomy Reports, 2014, Vol. 58, No. 11, pp. 849–859. © Pleiades Publishing, Ltd., 2014.
Original Russian Text © A.I. Martynova, V.V. Orlov, 2014, published in Astronomicheskii Zhurnal, 2014, Vol. 91, No. 11, pp. 957–968.

Trajectories of Bodies in Zones of Rapidly Decaying Triple Systems

A. I. Martynova[1] and V. V. Orlov[2,3*]

[1]*St. Petersburg State Forestry University, St. Petersburg, Russia*
[2]*St. Petersburg State University, St. Petersburg, Russia*
[3]*Main (Pulkovo) Astronomical Observatory, Russian Academy of Sciences, St. Petersburg, Russia*

Received July 30, 2013; in final form, May 21, 2014

Abstract—The general three-body problem with equal masses and zero initial velocities is considered. Zones in which the triple systems decay over short times $T < 10T_{\rm cr}$ are distinguished in the domain of the initial conditions, where $T_{\rm cr}$ is the mean crossing time for a component of the triple system. These zones form distinct families of structures. Properties of the trajectories of bodies within these structures are described. The structures often display a layered character, with each layer corresponding to triple systems in which a particular body departs during the decay. These layers alternate with zones in which the decay does not occur on such short time scales, and the bodies are flung outward without this leading to a departure, or undergo simple interactions. In the zones of rapid decay, the departure of one of the bodies occurs after one or a few triple encounters between the components.

DOI: 10.1134/S1063772914110031

1. INTRODUCTION

The gravitatioinal three-body problem was formulated by Newton at the end of the 17th century, and has since attracted the attention of many eminent researchers in mathematics, mechanics and astronomy. A number of interesting analytical and qualitative results concerning the motion of the components have been obtained. However no fully acceptable solution has been obtained, in spite of the application of enormous efforts (a review of analytical studies of the three-body problem can be found in [1]). Over the last decades, a number of researchers have engaged in numerical simulations as a means of studying the dynamics of triple systems (see, e.g., [2, 3]).

The first numerical simulations of the three-body problem with equal masses and zero initial velocities (the so-called free-fall three-body problem) were carried out by Agekyan and Anosova [4] in 1967. The main result of that work was that the evolution of such triple systems always ends in decay, with one of the components departing along a hyperbolic orbit, leaving behind a binary formed by the other two bodies. This fundamental result was later confirmed in a number of other studies, and generalized to the case of components of unequal masses (see references in [2, 3]).

Agekyan and Anosova [4, Fig. 2] presented trajectories of bodies in triple systems from the initial time to the decay of the system. These trajectories are very complex and tangled. Binary and triple encounters occur, and components are flung away from the center of mass and undergo complex interactions. The evolution of a triple system ends in decay following a close triple encounter of the bodies. One glance at the trajectories in this figure makes it clear why it is so difficult to obtain an analytical representation for the trajectories of the three bodies. Nevertheless, a detailed analysis of the character of the motions of the bodies enables the identification of a number of interesting properties of the orbits (see, e.g., [5, 6]). A classification of the various possible states in the general three-body problem was proposed based on an analysis of the trajectories of Szebehely [7] and Agekyan and Martynova [8], and criteria for triple encounters, simple interactions, and component ejections were obtained.

In the current study, we have investigated the trajectories of bodies in the free-fall three-body problem in the case of rapidly decaying triple systems, and have identified characteristic properties of the dynamical evolution of such systems.

2. FORMULATION OF THE PROBLEM

This study continues the work of [9]. As in [9], we consider a triple system with components of equal mass having zero initial velocity. We used the method for specifying the initial conditions proposed in [4]. At the initial time, the first body A is located at the

*E-mail: vorvor1956@yandex.ru

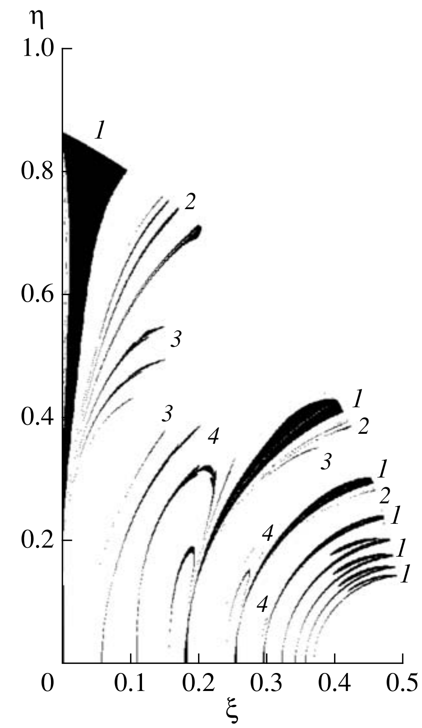

Fig. 1. Initial coordinates (ξ, η) for triple systems with lifetimes $T < 10T_{\text{cr}}$.

point with coordinates $(-0.5, 0)$, the second body B at the coordinates $(+0.5, 0)$, and the third body C at the coordinates (ξ, η) inside a domain D bounded by the coordinate axes and the arc of a circle of unit radius with its center at the point $(-0.5, 0)$. As was shown in [4], this method for specifying the initial conditions encompasses all possible configurations of the triple systems. Since the angular momentum of the triple system is zero, the motion will proceed in the plane of the initial triangular configuration.

As in [9], we used the following system of dynamical units:

(1) the unit of distance was taken to be the mean size of the triple system,

$$d = \frac{G\sum_{i<j} m_i m_j}{|E|},$$

where G is the gravitational constant, $m_i (i = 1, 2, 3)$ are the masses of the bodies, and E is the total energy of the triple system;

(2) the unit of time was taken to be the mean crossing time for a component of the triple system,

$$T_{\text{cr}} = \frac{\sqrt{G}(\sum_{i=1}^{3} m_i)^{5/2}}{(2|E|)^{3/2}}.$$

We adopted units such that $G = 1$, and the masses of the bodies were also taken to be unity.

In [9], we identified triple systems with various decay times T according to the criterion of Standish [10]. We consider here triple systems with short lifetimes, $T < 10T_{\text{cr}}$. To study the character of the motions of the bodies in such systems in more detail, we numerically integrated the equations of motion of the general three-body problem in barycentric coordinates (the coordinate origin was located at the center of mass of the triple system). We applied the method of Bulirsch and Stoer [11] to numerically solve the system of differential equations. We reduced the uncertainties during close binary encounters using the regularization technique of Aarseth and Zare [12]. All calculations were carried out using Aarseth's code TRIPLE [13]. When constructing individual trajectories, we specified tolerance parameter $\varepsilon = 3 \times 10^{-16}$.

3. RESULTS

Zones of rapid decays were distinguished in the domain D of the initial conditions (ξ, η) [9]. These often correspond to triple systems whose decays occur after the first close triple encounter, preceded by n binary encounters of components B and C: $n = 0, 1, 2, \ldots$ These zones form a system of arcs concentrated toward the lower-right corner of the domain D. This system of arcs is clearly visible in Fig. 1, which shows the points (ξ, η) corresponding to triple systems with decay times $T < 10T_{\text{cr}}$. In addition to this system of arcs, other systems of zones with more complex structures are also observed, in which the triple systems also decay over comparatively short times after a small number of triple encounters. Qualitatively, these structures correspond to zones of departure following the first, second, and third triple encounter found by Tanikawa and Umehara [6].

The studies of the trajectories of bodies in individual zones of rapid departures considered in [5, 9] showed the complex structure of these zones. The zones of departure following the first triple encounter, which are concentrated toward the lower-right corner of the domain D, have a layered structure. Three layers correspond to the departures of one of the three bodies after the first triple encounter; in two separating layers, there is no departure after the first triple encounter, and there are ejections of bodies and simple interaction states according to the classification of Agekyan and Martynova [8].

Let us consider in more detail the trajectories of bodies in the individual layers in the zones of rapid decay with $T < 10T_{\text{cr}}$, beginning with the system of arcs concentrated toward the lower-right corner of the domain D (Fig. 1). Figure 1 shows eight such zones (indicated by the number *1*). The first zone is concentrated toward the vertical axis, while the remaining zones converge toward the lower-right

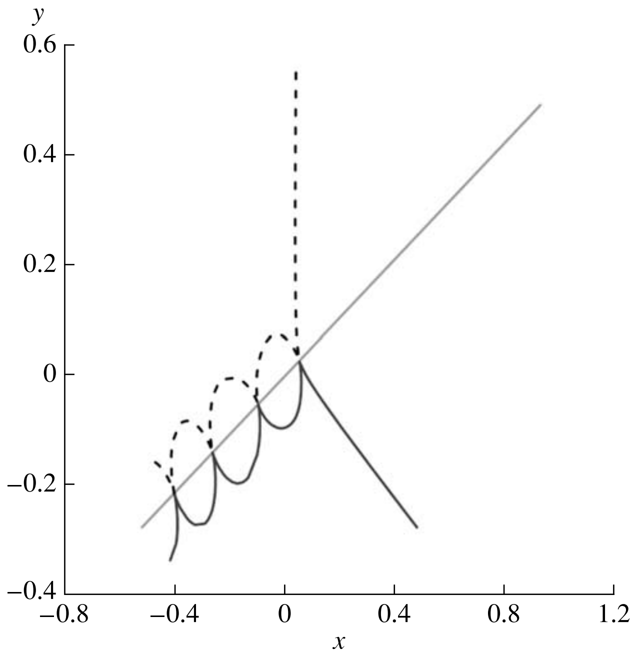

Fig. 2. Trajectories of bodies in a triple system with initial coordinates $(\xi, \eta) = (0.06, 0.828)$ over a time $t = 1.0T_{\rm cr}$.

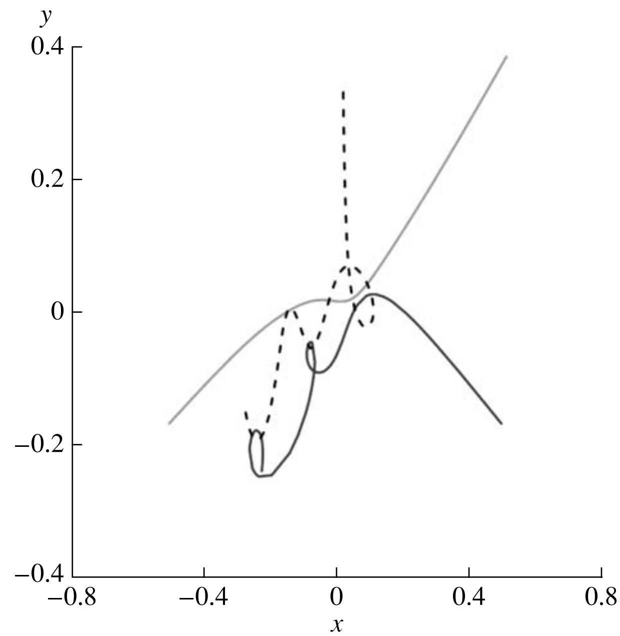

Fig. 3. Trajectories of bodies in a triple system with initial coordinates $(\xi, \eta) = (0.024, 0.5)$ over a time $t = 1.5T_{\rm cr}$.

corner of the domain D. Note that the pattern does not end with the eighth zone, but the decay times for the subsequent zones are $T > 10T_{\rm cr}$, and so are not considered in this study. As was shown in [5] and confirmed in [9], the zones of rapid departure from this family are dynamically equivalent, and differ only in the number of binary encounters of components B and C before the close triple encounter that leads to the departure of one of the three components. The number n of binary encounters is one less than the zone number when the zones are counted from the vertical axis toward the right: the triple encounter occurs immediately in the first zone, is preceded by one binary encounter in the second zone, is preceded by two binary encounters in the third zone, etc.

The internal structure of each zone is analogous to the structures discussed in [5, 9], where the following sequence was shown. When moving within each zone from left to right along the 0ξ axis at fixed η, the departure of component B after its passage through the center of mass of the pair AC is first observed. Further, there is a narrow transition zone in which there is no decay of the triple system after the first triple encounter. This is followed by a narrow zone in which component C undergoes an encounter with the center of mass of the AB pair, reverses its motion, and departures in a directly roughly opposite to its original direction of approach. Further, there is another narrow transition zone in which there is no decay of the triple system after the first triple encounter, followed by a zone corresponding to the departure of component A after its passage through the center of mass of the BC pair. As was noted in [9], the central zone corresponding to the departure of component C does not reach the $O\xi$ axis, and ends somewhat before this. This is so because, in the limiting case $\eta = 0$, we are dealing with the rectilinear three-body problem, in which the departure of the central body is not possible.

In scanning along some zone from top to bottom, the angle along which an ejected component moves relative to the direction of its motion before the triple encounter changes. In the upper part of the zone near the circular arc $(\xi + 0.5)^2 + \eta^2 = 1$ that bounds the domain D on the right, the departing body A moves along a nearly linear orbit (Fig. 2). When moving downward in the zone, the angle between the directions of arrival into the triple encounter and of the emergence from this encounter increases (Fig. 3). The trajectory of the departing body displays an inflection near the coordinate origin. The second derivative of the coordinates of the passing body with respect to either of its coordinate changes sign at the location of this bend.

Beginning with the fifth zone, we observe a small "spur" in the upper part of the zone, directed outward relative to the point $\xi = 0.5, \eta = 0$. Analysis of trajectories with initial conditions within such spurs indicates that an exchange triple encounter according

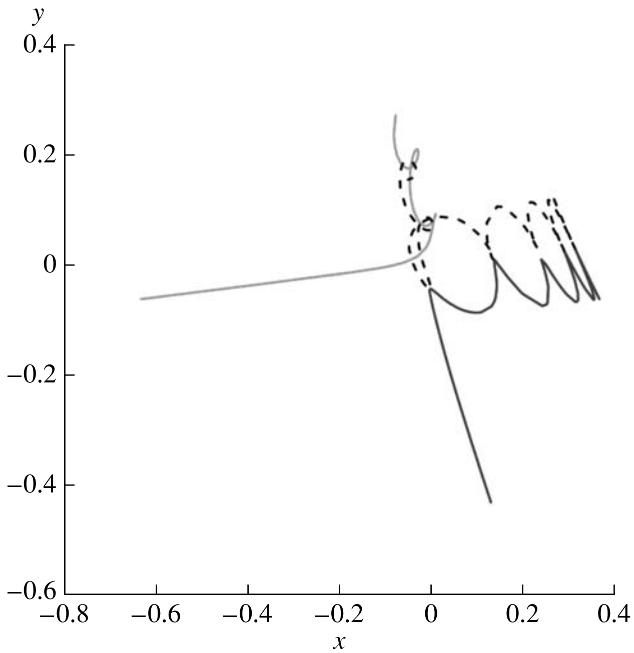

Fig. 4. Trajectories of bodies in a triple system with initial coordinates $(\xi, \eta) = (0.401, 0.182)$ over a time $t = 2.5T_{\rm cr}$.

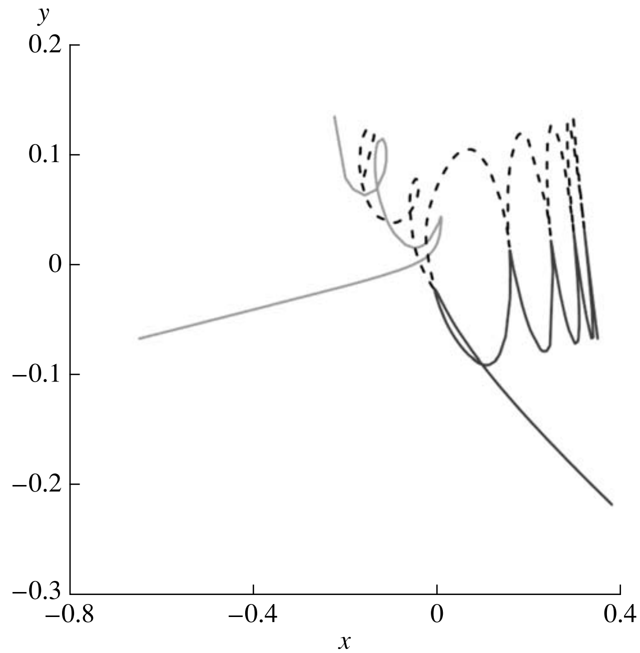

Fig. 5. Trajectories of bodies in a triple system with initial coordinates $(\xi, \eta) = (0.447, 0.2)$ over a time $t = 2.5T_{\rm cr}$.

to the classification of Anosova and Zavalov [5] occurs after n binary encounters of components B and C, leading to the departure of component B. Figure 4 shows an example of such a trajectory for $n = 4$ (fifth zone) with its initial conditions in the lower part of the spur. Another example for initial conditions in the upper part of the spur is presented in Fig. 5. In both cases, the result of the final triple encounter that leads to the decay of the triple system is the departure of component B. The triple encounter consists of two binary encounters of component C, first with A and then with B. As a result, component B acquires additional kinetic energy, which proves to be sufficient for it to escape from the triple system. Components A and C form the final binary system.

Note that the system of concentric arcs and adjacent spurs was identified by Tanikawa and Umehara [6] as a system of regions in which the decay of the triple system occurs after the first close triple encounter of the components. It was shown in [6] that lines of binary collisions, as well as points of triple collisions lying on the circle $(\xi + 0.5)^2 + \eta^2 = 1$ forming the right boundary of the domain D, are associated with the concentric zones. In the first zone adjacent to the vertial axis, the triple-collision point $\xi = 0, \eta = \sqrt{3}/2$ is located at the apex of an equilateral triangle. Anosova and Zavalov [5] noted that the components are also often located near the apex of an equilateral triangle before they enter into a close triple encounter. The triple encounter itself occurs in the vicinity of the triple collision.

In addition to the systems of concentric zones and spurs discussed above, other regions of initial conditions (ξ, η) in which the triple systems rapidly decay can be identified in Fig. 1. Let us consider the motions of bodies in the zones denoted *2* in Fig. 1. Examples of trajectories from these zones are shown in Figs. 6–8. The initial points (ξ, η) are located near the boundary of the domain D. Consequently, the motions of the bodies are close to the corresponding motions in the plane of the isosceles problem, i.e., the generalized problem of Sitnikov. First there is a wide triple encounter of component A with the center of mass of the BC pair, after which component A reverses its motion and a second close flyby triple encounter [5] occurs. Further, component A departs from the triple system along a nearly linear orbit. The differences in the trajectories in Figs. 6–8 consist of different numbers of binary encounters of B and C between the first wide triple encounter and the second close triple encounter.

Similar structures are also observed after the second and third zones from Family *1*. These are denoted by the number *2* in Fig. 1. Similar structures may also be present after the subsequent zones of the first family. Verifying this requires more detailed scanning of the vicinity of the lower-right corner of the domain D. Figure 9 presents an example of the evolution of a triple system with initial conditions from the second

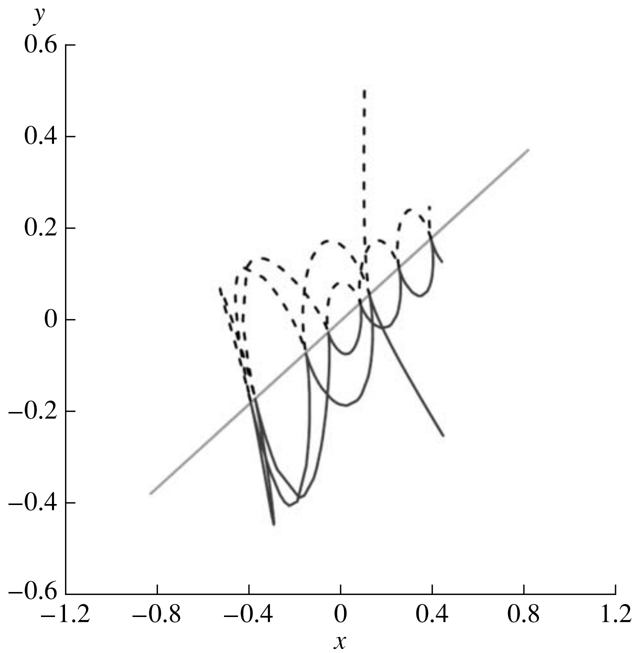

Fig. 6. Trajectories of bodies in a triple system with the initial coordinates $(\xi, \eta) = (0.156, 0.754)$ over a time $t = 3.2T_{\rm cr}$.

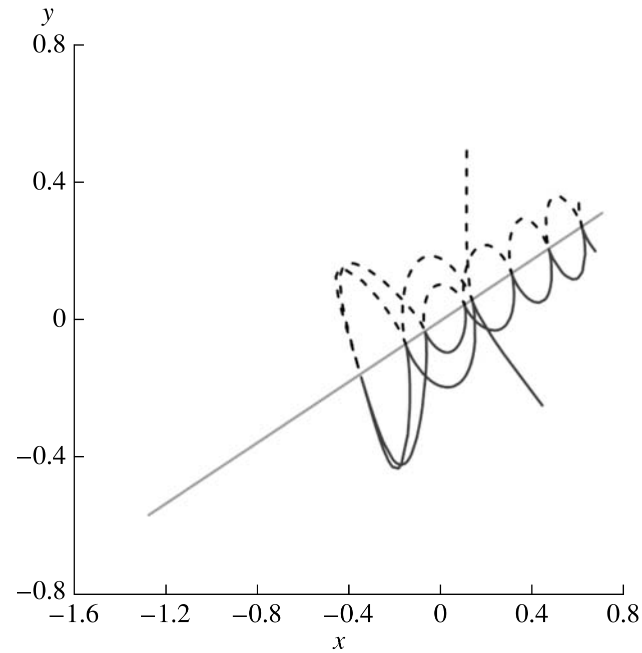

Fig. 7. Trajectories of bodies in a triple system with the initial coordinates $(\xi, \eta) = (0.17, 0.742)$ over a time $t = 3.2T_{\rm cr}$.

system of zones in Family *2*. The difference from the trajectories of the first system of zones of Family *2* shown in Figs. 6–8 is that one binary encounter of B and C in the first system of zones and two binary encounters of these bodies in the second system of zones occurs before the first triple encounter. Thus, the number of binary encounters preceding the first triple encounter increases in steps of unity as we move to the right.

A sequence of triple-collision points discovered in [6] is associated with the zones of rapid decay from the Family *2*. The zones of departure of various bodies after close triple encounters in the vicinity of a given collision and intermediate layers in which there is no departure of a body after a close triple encounter converge in the vicinity of these points [6, Fig. 3]. Tanikawa and Umehara [6] suggest that the circle $(\xi + 0.5)^2 + \eta^2 = 1$ bounding the region D on the right has an infinite sequence of triple-collision points corresponding to the various zones of Family *2*. These sequences repeat after each of the zones of Family *1*. Just as in each zone from Family *1*, there is one triple-collision point lying on the same boundary of the domain D. We suppose that these triple-collision points also form an infinite sequence converging toward the lower-right corner of the domain D, i.e., toward the point $\xi = 0.5$, $\eta = 0$. Thus, we expect that the number of triple-collision points at the right boundary of the domain D forms an infinite countable set. The situation inside the domain D is apparently more complex; this can be elucidated using symbolic-dynamics methods (see, for example, [14–16]).

Let us now turn to the other zones of rapid de-

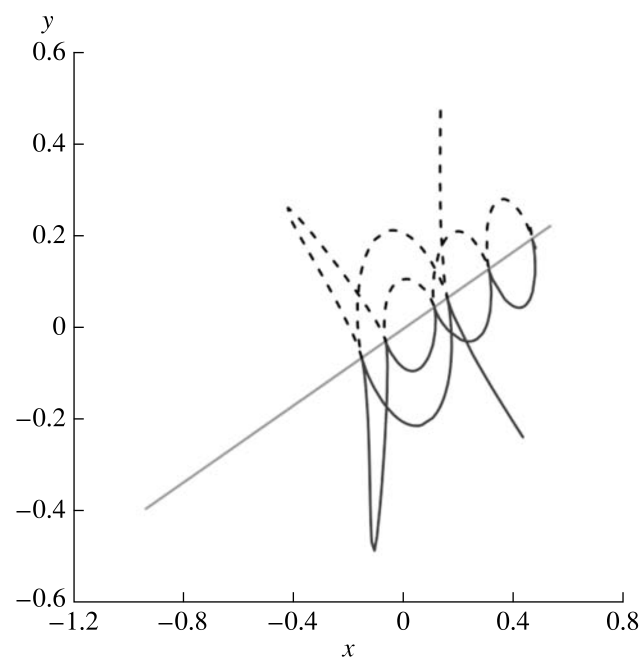

Fig. 8. Trajectories of bodies in a triple system with the initial coordinates $(\xi, \eta) = (0.2, 0.714)$ over a time $t = 2.5T_{\rm cr}$.

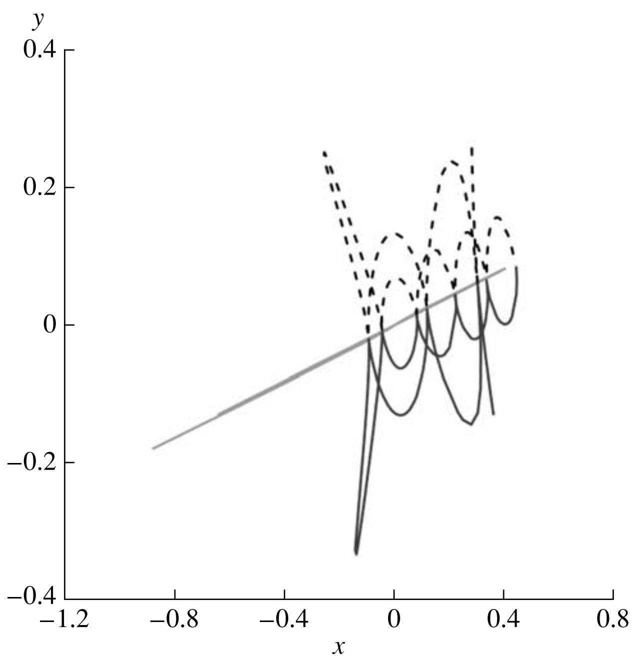

Fig. 9. Trajectories of bodies in a triple system with the initial coordinates $(\xi, \eta) = (0.421, 0.387)$ over a time $t = 3.0T_{\rm cr}$.

parture observed in Fig. 1. First and foremost, this corresponds to the zones in Family *3*. An example of the evolution of a system from this family is shown in Fig. 10. Since the zones from Family *3* do not reach the right boundary of the domain D, the motions of these triple systems deviate strongly from the isosceles case. Component C departs at the apex of the zone (Fig. 10) after a wide flyby triple encounter, resembling the first triple encounter in the systems from Family *2*. A series of binary encounters of various pairs is followed by the final close triple encounter of component C with bodies A and B. With movement downward along the zone, it separates into several layers. With movement from left to right along the ξ axis with fixed η, we first encounter a region where body A departs (a typical example is shown in Fig. 11), followed by a layer without a departure after the second triple encounter, the departure of component C at the center of the zone (Fig. 12), another layer without a departure after the second triple encounter, and finally a layer corresponding to the departure of component B after it passes through the center of mass of the AC pair (Fig. 13).

A similar situation is observed for the other zones of Family *3* located to the right of the first zone. The only difference is the number of binary encounters of components A and C preceding the close triple encounter that leads to the departure of one of the components. Comparing Figs. 14 and 10, which depict the evolution of systems with initial conditions at the apices of the second zone and first zone, respectively, we can see that the evolution proceeds

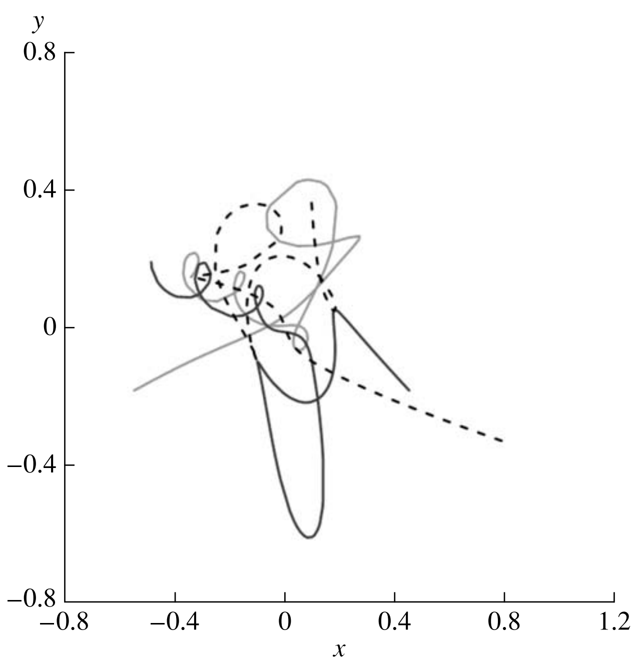

Fig. 10. Trajectories of bodies in a triple system with the initial coordinates $(\xi, \eta) = (0.145, 0.547)$ over a time $t = 3.0T_{\rm cr}$.

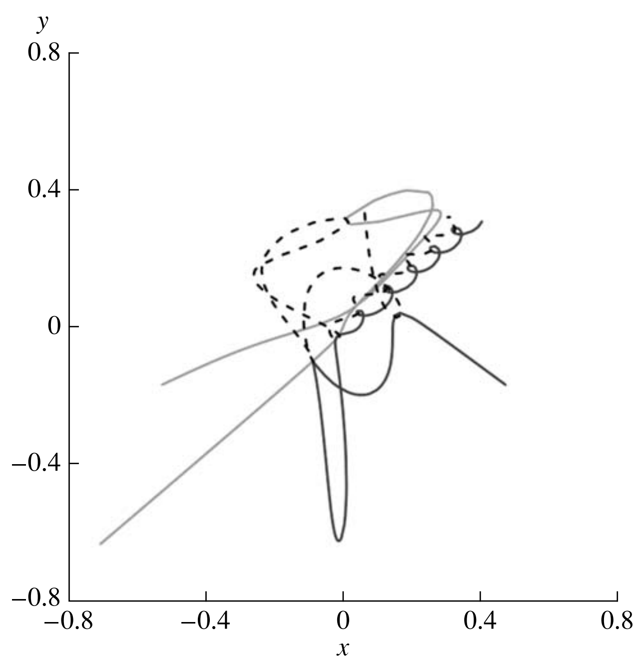

Fig. 11. Trajectories of bodies in a triple system with the initial coordinates $(\xi, \eta) = (0.09, 0.5)$ over a time $t = 3.0T_{\rm cr}$.

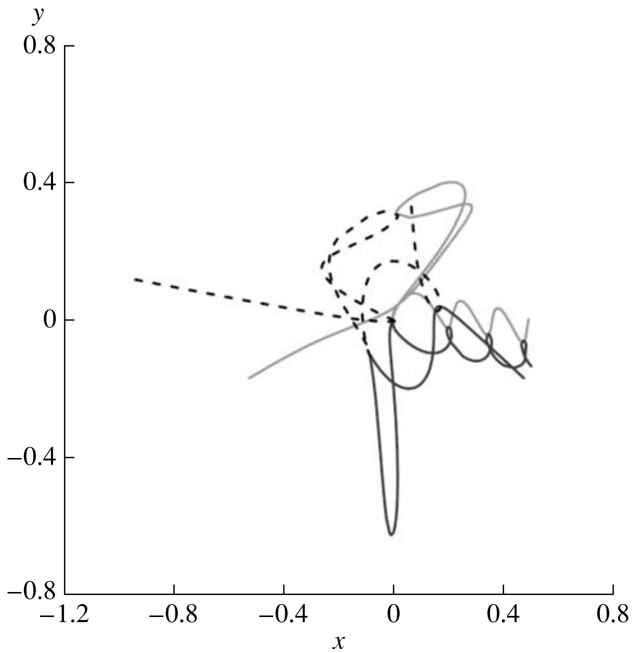

Fig. 12. Trajectories of bodies in a triple system with the initial coordinates $(\xi, \eta) = (0.0906, 0.5)$ over a time $t = 3.0T_{\rm cr}$.

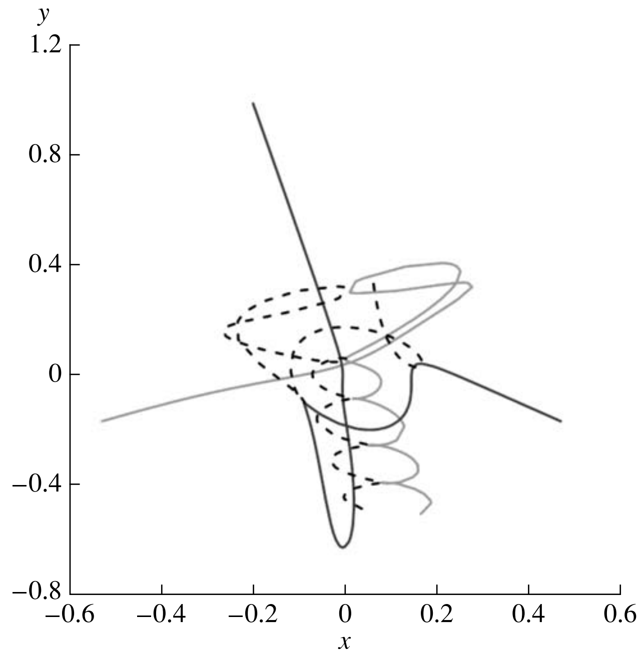

Fig. 13. Trajectories of bodies in a triple system with the initial coordinates $(\xi, \eta) = (0.092, 0.5)$ over a time $t = 3.0T_{\rm cr}$.

according to the same scenario in both cases. At the end of the evolution, component C leaves the triple system after undergoing a succession of close binary encounters with components B and A and the final close triple encounter that leads to the decay of the system. A similar situation also pertains to the third zone of this family, located to the right of the second zone. Figure 15 shows that component C likewise departs at the apex of the third zone, but the final close triple encounter is preceded by three binary encounters of components A and C. We expect that there also exist other zones in Family *3* in which the final triple encounter is preceded by larger numbers of binary encounters of A and C. These additional zones should be located to the right of the third zone in Family *3*.

We expect that analogous systems of zones from Family *3* are located after each zone from Family *1*. The first such zone from the second system of zones located to the right of the second zone from Family *1* can be seen in Fig. 1, where it is denoted *3*. The only difference between these systems of zones from Family *3* is the number of binary encounters of bodies B and C preceding the first wide triple encounter. The number of such binary encounters is equal to the number of the zone system. Only two zone systems from Family *3* are visible in Fig. 1. Since the decay times of the triple systems in the subsequent systems of zones from this family exceed $10T_{\rm cr}$, they were not included in this figure.

Let us now consider the last family of zones of

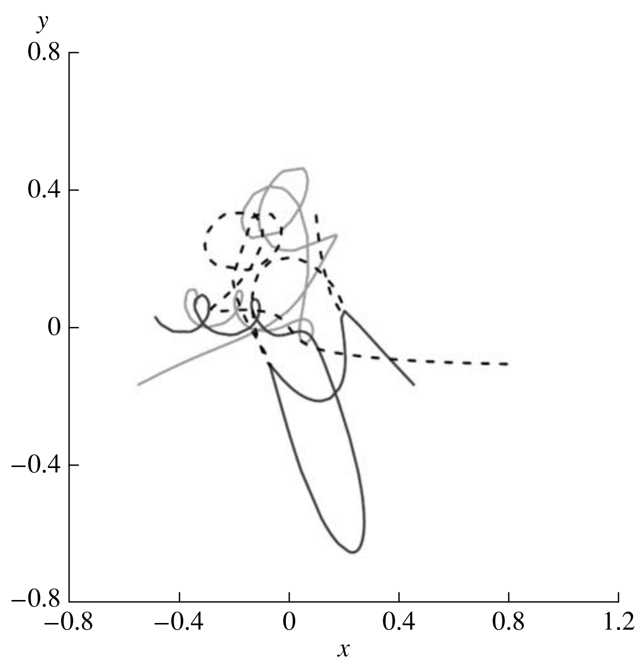

Fig. 14. Trajectories of bodies in a triple system with the initial coordinates $(\xi, \eta) = (0.145, 0.493)$ over a time $t = 3.3T_{\rm cr}$.

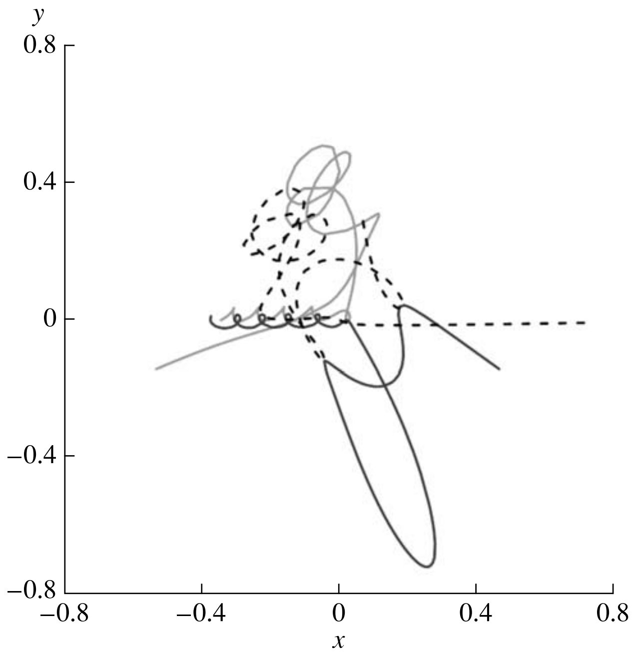

Fig. 15. Trajectories of bodies in a triple system with the initial coordinates $(\xi, \eta) = (0.103, 0.432)$ over a time $t = 3.5T_{\rm cr}$.

rapid decay depicted in Fig. 1: Family *4*. The main structure in this family consists of two parts: an upper "cap" and lateral "legs," leading to the 0ξ axis from the left in the lower part and adjacent to the second zone of Family *1* on the right. Analysis of the trajectories of the bodies for specified initial conditions (ξ, η) inside the cap shows that body C departs in all cases. An example of such a trajectory is shown in Fig. 16. The evolution of the triple system consists of a series of binary encounters, first between B and C, then between A and C, B and C, and again A and C. This series of binary encounters is followed by a triple encounter consisting of rapidly alternating binary encounters of the departing component C with each of the remaining bodies B and A.

A similar character of the evolution is observed on the lateral branches of this zone. However, the result of the last triple encounter depends on the arrangement of the initial point inside the branch. The same five layers as in the zones of Family *1* are observed: three layers corresponding to departures of B, C, and A (from left to right) and two intermediate layers in which there is no departure after the triple encounter. The same pattern is observed in the right branch, with only the order of the departing bodies changed: A, C, and B (from left to right). Thus, component A departs after the triple encounter in the inner part of the lateral zones, component B in the outer part, and component C in the central part and in the cap.

There is another zone of rapid departures inside the main zone of Family *4*, with the same form as the main zone of this family, but smaller in size. Figure 17

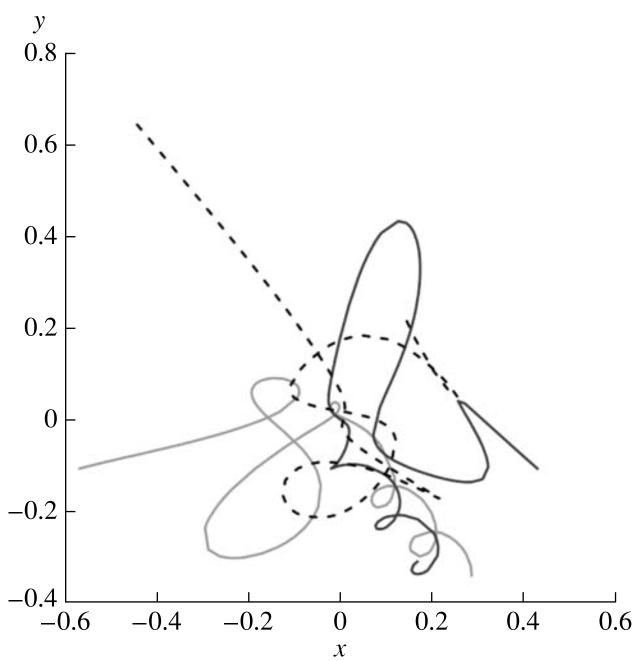

Fig. 16. Trajectories of bodies in a triple system with the initial coordinates $(\xi, \eta) = (0.215, 0.323)$ over a time $t = 3.0T_{\rm cr}$.

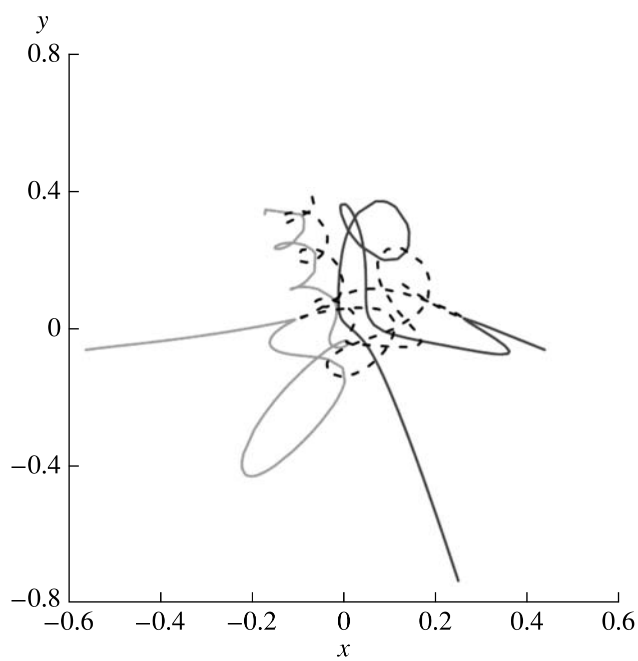

Fig. 17. Trajectories of bodies in a triple system with the initial coordinates $(\xi, \eta) = (0.191, 0.191)$ over a time $t = 3.5T_{\rm cr}$.

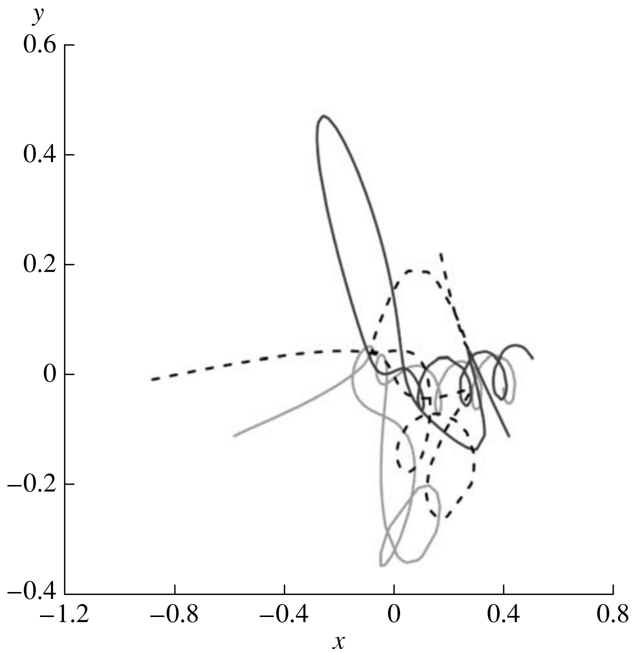

Fig. 18. Trajectories of bodies in a triple system with the initial coordinates $(\xi, \eta) = (0.252, 0.331)$ over a time $t = 3.5T_{\rm cr}$.

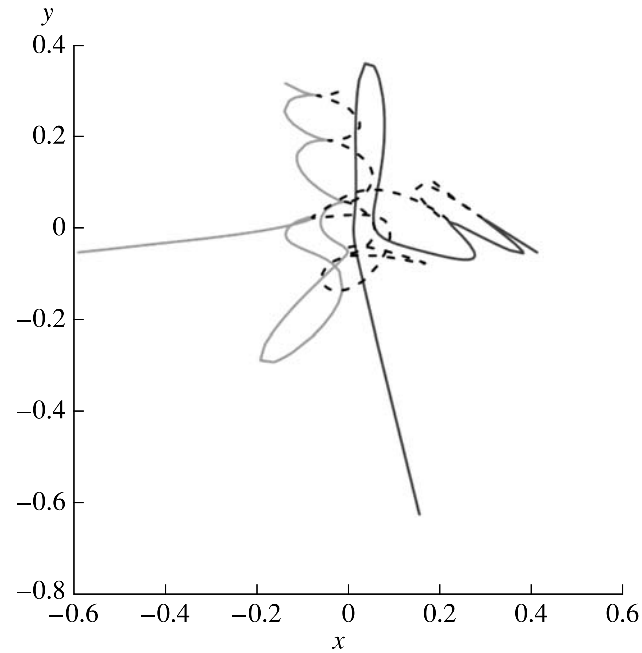

Fig. 19. Trajectories of bodies in a triple system with the initial coordinates $(\xi, \eta) = (0.275, 0.154)$ over a time $t = 3.5T_{\rm cr}$.

presents an example of a trajectory from this zone (see for comparison Fig. 16). Analysis of the character of the motions in this zone shows that the trajectories resemble those in the main zone at the start of their evolution, but include an additional binary encounter of bodies B and C (in the upper-right corner) before the close triple encounter that leads to the decay of the system.

There is also a zone of rapid departures outside the main zone, consisting of two lateral parts surrounding the main zone on the left and right (no rapid departures were found in the central part). Figure 18 shows an example of a trajectory from this zone (see for comparison Fig. 16). For given initial conditions, the beginning of the evolution of a triple system in this zone also resembles the motions in the main zone, but another binary encounter of components A and C (in the lower-left corner) is observed prior to the triple encounter leading to the decay of the triple system. We suppose that there are also other zones both inside and outside the main zone of Family *4*, in which the number of binary encounters of bodies B and C or A and C preceding the final triple encounter is even higher. Such zones could be manifest if we increased the limiting decay time and considered systems with $T > 10T_{\rm cr}$.

Note also that the zones of rapid decay from Family *4* appear in Fig. 1 in the vicinity (to the left) of the third and fourth zones of Family *1* (these zones are denoted *4*). The evolution of the triple systems in these zones recalls the evolution in the zones considered above to the left of the second zone of Family *1*. The difference is that additional binary encounters of components B and C occur at the beginning of the evolution. The number of such binary encounters is one fewer than the number of the neighboring zone from Family *1*. This is illustrated by the evolution of a triple system from the zone of rapid decays of Family *4* shown in Fig. 19, located in the vicinity (to the left) of the third zone of Family *1* (see for comparison Fig. 16). Note, however, that there is no "cap" distinct in the main zone of Family *4* in this case.

4. CONCLUSION

Thus, we have identified four main families of zones of rapid departures (Fig. 1) in the general three-body problem with equal masses and zero initial velocities (the free-fall three-body problem). For Families *1* and *2*, an important role is played by the right boundary of the domain D of all possible configurations—the circle $(\xi + 0.5)^2 + \eta^2 = 1$. Triple-collision points associated with the corresponding zones of rapid departure are located at this boundary [6]. In addition to these triple-collision

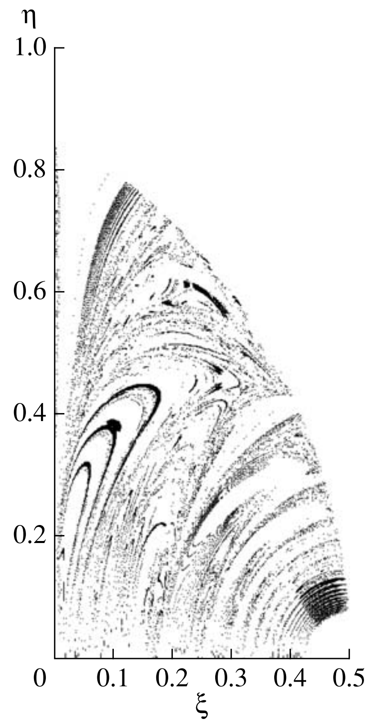

Fig. 20. Initial coordinates (ξ, η) for triple systems with lifetimes $20T_{\rm cr} > T > 10T_{\rm cr}$.

points, there is another triple-collision point inside the domain D in each zone of Families *1* and *2*. The lines of binary collisions for specified pairs of bodies pass inside the zones. These points and lines were identified by Tanikawa and Umehara [6].

In the zones of Family *1*, the departure always occurs after the first close triple encounter between the components, while it occurs after the second triple encounter in the zones of Family *2*. The close triple encounter leading to the decay of the triple system can be preceded by various numbers of binary encounters. The initial conditions corresponding to a specified number of binary encounters of a specified pair of bodies in a particular order form separate zones in the domain D. The internal structure of the zones is apparently determined by the triple-collision points, where the regions of departure of various bodies converge, alternating with regions in which there is no departure following a given triple encounter. As a result, the zones have the layered structure described above.

The zones of Families *3* and *4* do not reach the right boundary of the domain D. In these zones, the departure of one of the bodies occurs after the second close triple encounter of the components. As in the zones of Families *1* and *2*, each zone of Families *3* and *4* is associated with a line on which the initial conditions corresponding to binary and triple collisions lie. These points and lines were also identified by Tanikawa and Umehara [6]. It seems likely that binary and triple collisions determine the internal structure of the zones of Families *3* and *4* to a considerable extent. In particular, a layered structure similar to that of the zones of Families *1* and *2* is observed in some zones, with regions of departures of certain bodies alternating with zones in which such departures are absent.

Each of the Families *2–4* apparently consists of a system of zones separated by the zones of Family *1*. The dynamical evolution of the triple systems in these systems of zones essentially repeats. The difference between the different systems of zones in the same family consists in different numbers of binary encounters of components B and C in the initial stage of the evolution. This suggests that the number of systems of zones in each of Families *2*, *3*, and *4* is countable, as is the number of zones in Family *1*: each arc-like zone from Family *1* corresponds to a single system of zones from Families *2–4*.

This raises the question of whether other families of zones of decay of triple systems after some number of triple encounters exist in the free-fall three-body problem. Answering this question requires further detailed studies of the trajectories of bodies in triple systems with decay times $T > 10T_{\rm cr}$. Figure 20 presents the initial positions (ξ, η) of triple systems with $20T_{\rm cr} > T > 10T_{\rm cr}$. A detailed analysis of the trajectories in these systems could elucidate this question, and also provide a deeper understanding of the dependence of the results for the evolution of a triple on the initial conditions.

ACKNOWLEDGMENTS

This work was supported by the Russian Foundation for Basic Research (grant no. 12-02-00185-a).

REFERENCES

1. C. Marchal, *The Three-Body Problem* (Elsevier, Amsterdam, 1990).
2. M. Valtonen and H. Karttunen, *The Three-Body Problem* (Cambridge Univ. Press, Cambridge, 2006).
3. A. I. Martynova, V. V. Orlov, A. V. Rubinov, L. L. Sokolov, and I. I. Nikiforov, *Dynamics of Triple Systems* (SPb. Gos. Univ., St. Petersburg, 2010) [in Russian].
4. T. A. Agekyan and Zh. P. Anosova, Sov. Astron. **11**, 1006 (1967).
5. Zh. P. Anosova and N. N. Zavalov, Sov. Astron. **33**, 79 (1989).

6. K. Tanikawa and H. Umehara, Celest. Mech. Dyn. Astron. **70**, 167 (1999).
7. V. Szebehely, Celest. Mech. **4**, 116 (1971).
8. T. A. Agekyan and A. I. Martynova, Vestn. Leningr. Univ., Ser. 1, No. 1, 122 (1973).
9. A. I. Martynova and V. V. Orlov, Astron. Zh. **91** (2014, in press).
10. E. M. Standish, Celest. Mech. **4**, 44 (1971).
11. R. Bulirsch and J. Stoer, Num. Math. **8**, 1 (1966).
12. S. J. Aarseth and K. Zare, Celest. Mech. **10**, 185 (1974).
13. S. J. Aarseth, *Gravitational N-Body Simulations. Tools and Algorithms* (Cambridge Univ. Press, Cambridge, 2003).
14. V. Orlov, A. Petrova, A. Rubinov, and A. Martynova, ASP Conf. Ser. **316**, 70 (2004).
15. A. Chernin, A. Martynova, A. Myllari, and V. Orlov, Ann. Univ. Turkuensis., Ser. 1A **358**, 16 (2006).
16. K. Tanikawa and S. Mikkola, Private commun. (2013).

Translated by D. Gabuzda